Parameter estimation of solar cells using datasheet information with the application of an adaptive differential evolution algorithm

Partha P. Biswas [a, *], P.N. Suganthan [a], Guohua Wu [b, **], Gehan A.J. Amaratunga [c]

[a] School of Electrical and Electronic Engineering, Nanyang Technological University, Singapore
[b] School of Traffic and Transportation Engineering, Central South University, Changsha, PR China
[c] Department of Engineering, University of Cambridge, UK

A R T I C L E   I N F O

A B S T R A C T

A solar cell or photovoltaic (PV) module is electrically represented by an appropriate circuit model with certain defined parameters. The parameters are required to be correctly computed from solar cell characteristic and/or a set of experimental data for simulation and control of the PV system. However, experimental data or accurate characteristic data (i.e. current-voltage or I-V curve) of a PV module may not be readily available. The manufacturer of a PV system usually provides relevant information on open circuit, short circuit and maximum power points. Therefore, an alternate approach is to estimate the PV system parameters by utilizing the I-V characteristic data at these three major points. The process involves formulation and solution of complex non-linear equations from an adopted solar cell model. This paper proposes an application of an advanced adaptive differential evolution algorithm on the problem of PV module parameter estimation using minimum available information from the manufacturer datasheet by implementing single-diode and double-diode models. Linear population size reduction technique of success history based adaptive differential evolution (L-SHADE) algorithm is implemented to minimize the error of current-voltage relationships at the above-mentioned three important points defining the I-V characteristic. The algorithm facilitates evolution of solutions that result in almost zero error ($< 10^{-12}$) at these three major points. All relevant parameters of the PV cell are optimized by the algorithm without any assumption or predetermination of parameters. It is observed that a set of feasible solutions (parameters) is obtained for the PV module from multiple runs of the algorithm. The fact of attaining several probable solutions from datasheet information using few other metaheuristics is also discussed in this work.

1. Introduction

Depletion of fossil fuels, environmental regulation and carbon tax imposition in many countries force mankind to look for clean, replenishable sources of energy. Solar energy is a popular form of renewable energy as it is abundant and almost ubiquitous. The energy can be directly converted to electricity by photovoltaic (PV) system. The unit of a PV system is the PV cell. Normally, many PV cells are grouped together to form a PV module. The array of PV modules can directly feed small DC loads. However, converter is necessary for larger applications of the electricity generated by the PV system. For effective utilization, the PV device is needed to be operated at maximum power point (MPP). Therefore, a designer must know the appropriate model of a PV cell for the detailed study, simulation and analysis.

A PV cell is a p-n junction diode, typically represented with an equivalent electrical circuit [1]. Depending on the accuracy sought, the designer can assume a model with one, two or even more diodes. Single-diode model has been the most popular model due to its simplicity coupled with an acceptable level of accuracy in representing the I-V characteristic. Double-diode model accounts for the loss in the depletion region caused by the recombination of carriers [2]. Though three-diode model has been studied in literature [3,4], the model has not been so popular as increment in accuracy with this model is not high enough considering the escalation in complexity due to addition of one more diode [5]. No

* Corresponding author.
** Corresponding author.
E-mail addresses: parthapr001@e.ntu.edu.sg (P.P. Biswas), epnsugan@ntu.edu.sg (P.N. Suganthan), guohuawu.nudt@gmail.com (G. Wu), gaja1@hermes.cam.ac.uk (G.A.J. Amaratunga).

matter whatever circuit model is adopted for the PV system, finding the optimum circuit parameters requires solution of transcendental equations relating I-V characteristic of the PV device. For a single-diode model, the parameters to be found are the diode ideality factor (a), the photocurrent (I_{PV}), the reverse saturation current of the diode (I_O), the series resistance (R_S) and the parallel resistance (R_P). Population based metaheuristic methods have been very effective in solving non-linear, multimodal optimization problems. In recent years, several evolutionary algorithms (EAs) have been applied in finding optimal parameters of a PV cell. Usually an error function between the sets of experimental and the simulated I-V data of the PV system is minimized by the EAs to provide optimal cell parameters. Variants of particle swarm optimization (PSO) such as time varying acceleration coefficients PSO (TVACPSO) [6] and enhanced leader PSO (ELPSO) [7] were applied to the problem of finding PV cell parameters. Flower pollination algorithm (FPA) [8] and hybrid [9] of FPA and Nelder-Mead simplex methods showed promising results in minimizing the error function. An improved version of shuffled complex evolution algorithm (ISCE) that could enhance exploration and exploitation capability of the original algorithm was proposed in Ref. [10] and the same was implemented to PV cell parameter estimation problem. A self-adaptive weight was incorporated into JAYA algorithm [11] in attempting the same problem. Certain adjustments on control parameters of differential evolution (DE) were observed in Refs. [12,13] and the modified adaptive DE was applied to error minimization objective. Chaotic maps were infused in chaotic whale optimization algorithm (CWOA) [14] to compute and automatically adapt the internal parameters of the algorithm in solving the PV cell problem. The literature [6–14] utilized the experimental data of selected solar cells provided in Ref. [15] at various points of the I-V curves adopting single and/or double-diode models. Synthetic I-V data of various PV modules were generated to evaluate the performance of penalty-based DE in Ref. [16]. Experimental I-V data of various PV modules under different temperatures and irradiance levels were used to find the cell parameters adopting DE with integrated mutation strategy [17] and bacterial foraging optimization (BFO) [18] algorithm. Power-voltage curve of the PV system was exploited in Ref. [19] using imperialist competitive (ICA) algorithm. In all these publications, a reasonably large set of data was needed for parameter estimation of the PV module.

In general, the PV module manufacturers provide limited information on the system. A few articles proposed useful methods to estimate parameters based on datasheet information. Ref. [20] presented a comparison of parameter extraction techniques of crystalline and thin-film solar-cell modules using classical Gauss-Siedel method and analytical method. A comparative study using the iterative method and Lambert W function was exhibited in Ref. [21]. Literature [22] suggested a detailed mathematical model of the PV module focusing mainly on three major points of open circuit, short circuit and maximum power on I-V curve. The combination of analytical and metaheuristic methods was discovered in Refs. [23,24]. Some of the parameters of the PV system were found analytically while the remaining parameters were estimated using particle swarm optimization (PSO) [23] and genetic algorithm (GA) [24]. The nameplate data of solar cell were utilized in Ref. [25] for parameter extraction applying bacterial foraging algorithm. This paper presents PV module parameter extraction using datasheet information at three major points of I-V characteristic curve for monocrystalline, polycrystalline and thin-film solar cells. A few parameters have been identified analytically, while the remaining parameters are optimized using linear population size reduction technique of success history based adaptive differential evolution (L-SHADE) algorithm [26]. Similar approach in Ref. [23] considered only single-diode model. Again, Villalva et al. [22] used datasheet information with analytical derivation of only the series resistance (R_S) and parallel resistance (R_P) values in single-diode model assuming certain values for diode ideality factor (a). This study includes both single and double-diode models without assuming any parameter for the solar cells. A new error function considering I-V characteristic at the three major points is formulated such that the optimization algorithm comes up with multiple probable feasible solutions from different trial runs of the optimization algorithm. The literature [22–25] that used datasheet information (only on three major points) for parameter extraction did not enlighten on the possibility of multiple optimal solutions during optimization even under a defined condition of operating temperature and solar irradiance. The simple error function together with the algorithm proposed in this work could ensure zero error at all trial runs under standard test conditions (STC). SHADE [27] is a powerful variant of DE algorithm. Classical DE requires 3-control parameters to be user defined: scale factor (F), crossover rate (CR) and population size (Np). In SHADE, F and CR values are automatically adapted based on the success history of earlier generations. In L-SHADE, population size (Np) is also dynamic and it is observed that a reasonable population size generates good solutions. In summary, the performance of L-SHADE is not so much dependent on user-defined inputs. Further, SHADE and its variant L-SHADE have shown very promising results for optimization of discrete [28] and continuous variables [29,30]. Inspired by the growing application in power domain and its competitive performance, we employ L-SHADE algorithm for the PV cell parameter estimation. Finally, the problem with same objective (error function) is optimized employing some other well-known algorithms such as genetic algorithm (GA) [31], particle swarm optimization (PSO) [32], artificial bee colony (ABC) [33], moth swarm algorithm (MSA) [34] and grey wolf optimizer (GWO) [35]. The contributions of this work can be summarized as below:

- An error function utilizing datasheet information on three major points of the I-V characteristic of a PV cell is proposed.
- A combination of analytical and metaheuristic methods is implemented to single and double-diode cell models.
- All PV cell parameters are optimized for both single and double-diode models without presumption of any cell parameter.
- L-SHADE algorithm is applied to optimize the error function for different types of PV cells. A set of feasible parameters is obtained for a cell from multiple independent runs of the algorithm.
- The results are analyzed in detail and a comparison of L-SHADE algorithm with other equivalent metaheuristics is carried out on the problem of PV cell parameter estimation.

The organization of the rest of the paper is as follows. Section 2 includes circuit analyses of both single-diode and double-diode models of the PV modules. In section 3, L-SHADE algorithm is briefly presented. The objective function and application of the L-SHADE algorithm are described in section 4. Section 5 presents the simulation results and a detailed analysis. The comparison of results of L-SHADE algorithm and other metaheuristics is provided in section 6. The paper ends with concluding remarks in section 7.

2. Mathematical model and numerical data

This section presents an analysis of the equivalent circuits of an ideal PV cell and a PV module considering single-diode and double-diode models, followed by some useful numerical data used in present study.

2.1. Mathematical model

2.1.1. Model of an ideal PV cell

Fig. 1 shows the equivalent circuit of an ideal PV cell. The output current (I) of the ideal cell is:

$$I = I_{PV,cell} - I_D \qquad (1)$$

where $I_{PV,cell}$ is the photovoltaic current generated by the cell due to incident light and I_D is the diode current. The diode current (I_D) is expressed by Schokley diode equation and hence Eq. (1). can be rewritten to obtain I-V characteristic of the ideal cell as [22]:

$$I = I_{PV,cell} - I_{0,cell}\left[exp\left(\frac{qV}{akT}\right) - 1\right] \qquad (2)$$

where $I_{0,cell}$ is the reverse saturation current of the diode, q is the charge of an electron ($1.60217646 \times 10^{-19}$ Coulomb), k is the Boltzmann constant ($1.38064852 \times 10^{-23}$ Joules/Kelvin), T is the absolute temperature (in Kelvin) of the diode junction and a is the diode ideality factor.

In reality, several PV cells are connected either in series or parallel to form a PV module. Here, we consider N_C number of cells are connected in series. The series connection provides a greater output voltage. Subsequently, the equivalent circuits of more practical models of PV modules are discussed.

2.1.2. Single-diode model of the PV module

Fig. 2 exhibits the single-diode equivalent model of the PV module with N_C series-connected cells. I-V characteristic of the single-diode model of the PV module is given by Ref. [22]:

$$I = I_{PV} - I_O\left[exp\left\{\frac{q(V + R_S I)}{akN_C T}\right\} - 1\right] - \frac{V + R_S I}{R_P} \qquad (3)$$

where I_{PV} is the photocurrent, I_O is the reverse saturation current of the PV module; R_S and R_P are the equivalent series and parallel resistances, respectively. At open circuit point we have, $I = 0$ and $V = V_{OC}$ (say); then from Eq. (3). we obtain,

$$0 = I_{PV} - I_O\left[exp\left(\frac{qV_{OC}}{akN_C T}\right) - 1\right] - \frac{V_{OC}}{R_P} \qquad (4)$$

Therefore,

$$I_{PV} = I_O\left[exp\left(\frac{qV_{OC}}{akN_C T}\right) - 1\right] + \frac{V_{OC}}{R_P} \qquad (5)$$

At short circuit point $V = 0$ and $I = I_{SC}$ (say); then from Eq. (3). we obtain,

$$I_{SC} = I_{PV} - I_O\left[exp\left(\frac{qR_S I_{SC}}{akN_C T}\right) - 1\right] - \frac{R_S I_{SC}}{R_P} \qquad (6)$$
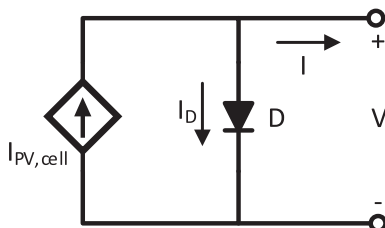
Therefore,

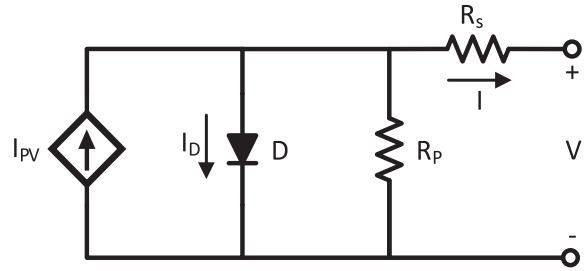Fig. 1. Equivalent circuit of an ideal PV cell.

Fig. 2. Equivalent circuit adopting single-diode model of a PV module.

$$I_{PV} = I_{SC} + I_O\left[exp\left(\frac{qR_S I_{SC}}{akN_C T}\right) - 1\right] + \frac{R_S I_{SC}}{R_P} \qquad (7)$$

From Eqs. (5) and (7). we find,

$$I_O = \frac{I_{SC} + \frac{R_S I_{SC}}{R_P} - \frac{V_{OC}}{R_P}}{exp\left(\frac{qV_{OC}}{akN_C T}\right) - exp\left(\frac{qR_S I_{SC}}{akN_C T}\right)} \qquad (8)$$

Substituting Eq. (8). into Eq. (5),

$$I_{PV} = \frac{\left(I_{SC} + \frac{R_S I_{SC}}{R_P} - \frac{V_{OC}}{R_P}\right)\left[exp\left(\frac{qV_{OC}}{akN_C T}\right) - 1\right]}{exp\left(\frac{qV_{OC}}{akN_C T}\right) - exp\left(\frac{qR_S I_{SC}}{akN_C T}\right)} + \frac{V_{OC}}{R_P} \qquad (9)$$

At maximum power point $V = V_{MPP}$ and $I = I_{MPP}$ (say); then from Eq. (3). we obtain,

$$I_{MPP} = I_{PV} - I_O\left[exp\left\{\frac{q(V_{MPP} + R_S I_{MPP})}{akN_C T}\right\} - 1\right] - \frac{V_{MPP} + R_S I_{MPP}}{R_P} \qquad (10)$$

2.1.3. Double-diode model of the PV module

The equivalent circuit adopting double-diode model for the PV module is shown in Fig. 3. I-V characteristic of the double-diode model is given by:

$$I = I_{PV} - I_{D1} - I_{D2} - \frac{V + R_S I}{R_P} \qquad (11)$$

i.e. $\quad I = I_{PV} - I_{01}\left[exp\left\{\frac{q(V + R_S I)}{a_1 kN_C T}\right\} - 1\right]$
$$- I_{02}\left[exp\left\{\frac{q(V + R_S I)}{a_2 kN_C T}\right\} - 1\right] - \frac{V + R_S I}{R_P} \qquad (12)$$

where I_{01} and I_{02} are the reverse saturation currents of the two diodes, a_1 and a_2 are their ideality factors. At open circuit point $I = 0$ and $V = V_{OC}$, therefore, from Eq. (12). we get:
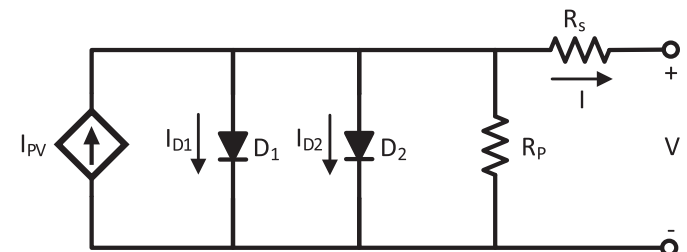

Fig. 3. Equivalent circuit adopting double-diode model of a PV module.

$$0 = I_{PV} - I_{O1}\left[exp\left(\frac{qV_{OC}}{a_1kN_CT}\right) - 1\right] - I_{O2}\left[exp\left(\frac{qV_{OC}}{a_2kN_CT}\right) - 1\right]$$
$$- \frac{V_{OC}}{R_P}$$
(13)

Therefore,

$$I_{PV} = I_{O1}\left[exp\left(\frac{qV_{OC}}{a_1kN_CT}\right) - 1\right] + I_{O2}\left[exp\left(\frac{qV_{OC}}{a_2kN_CT}\right) - 1\right] + \frac{V_{OC}}{R_P}$$
(14)

At short circuit point $V = 0$ and $I = I_{SC}$, therefore from Eq. (12). we get:

$$I_{SC} = I_{PV} - I_{O1}\left[exp\left(\frac{qR_SI_{SC}}{a_1kN_CT}\right) - 1\right] - I_{O2}\left[exp\left(\frac{qR_SI_{SC}}{a_2kN_CT}\right) - 1\right]$$
$$- \frac{R_SI_{SC}}{R_P}$$
(15)

Therefore,

$$I_{PV} = I_{SC} + I_{O1}\left[exp\left(\frac{qR_SI_{SC}}{a_1kN_CT}\right) - 1\right] + I_{O2}\left[exp\left(\frac{qR_SI_{SC}}{a_2kN_CT}\right) - 1\right]$$
$$+ \frac{R_SI_{SC}}{R_P}$$
(16)

From Eqs. (14) and (16). we find:

$$I_{O2} = \frac{I_{SC} + \frac{R_SI_{SC}}{R_P} - \frac{V_{OC}}{R_P} - I_{O1}\left[exp\left(\frac{qV_{OC}}{a_1kN_CT}\right) - exp\left(\frac{qR_SI_{SC}}{a_1kN_CT}\right)\right]}{exp\left(\frac{qV_{OC}}{a_2kN_CT}\right) - exp\left(\frac{qR_SI_{SC}}{a_2kN_CT}\right)}$$
(17)

Substituting Eq. (17) into Eq. (14):

$$I_{PV} = I_{O1}\left[exp\left(\frac{qV_{OC}}{a_1kN_CT}\right) - 1\right]$$
$$+ \frac{I_{SC} + \frac{R_SI_{SC}}{R_P} - \frac{V_{OC}}{R_P} - I_{O1}\left[exp\left(\frac{qV_{OC}}{a_1kN_CT}\right) - exp\left(\frac{qR_SI_{SC}}{a_1kN_CT}\right)\right]}{\left[exp\left(\frac{qV_{OC}}{a_2kN_CT}\right) - exp\left(\frac{qR_SI_{SC}}{a_2kN_CT}\right)\right]\left[exp\left(\frac{qV_{OC}}{a_2kN_CT}\right) - 1\right]^{-1}} + \frac{V_{OC}}{R_P}$$
(18)

At maximum power point $V = V_{MPP}$ and $I = I_{MPP}$ (say); then from Eq. (12). we obtain:

$$I_{MPP} = I_{PV} - I_{O1}\left[exp\left\{\frac{q(V_{MPP} + R_SI_{MPP})}{a_1kN_CT}\right\} - 1\right]$$
$$- I_{O2}\left[exp\left\{\frac{q(V_{MPP} + R_SI_{MPP})}{a_2kN_CT}\right\} - 1\right] - \frac{V_{MPP} + R_SI_{MPP}}{R_P}$$
(19)

2.2. Numerical data

This study considers three different types of polycrystalline, monocrystalline and thin film solar cell modules. The typical data provided by the manufactures are listed in Table 1. It is worthwhile to mention that current and voltage data at three major points (short circuit, open circuit and maximum power points) are explicitly given by the manufacturer at standard test conditions (STC) i.e. temperature 25 °C, irradiance 1000 W/m².

3. Linear population reduction technique of success history based adaptive differential evolution (L-SHADE) algorithm

Differential evolution (DE), a population based stochastic algorithm, is fast and reliable for optimization of non-linear, multimodal and constrained problems. The performance of DE vastly depends on 3-control parameters: the scaling factor (F), the crossover rate (CR) and the population size (Np), and also in addition, the selected mutation/crossover strategies [37]. Instead of fixed control parameters, dynamically adjusted parameters have shown superior performance. In success history based adaptive DE (SHADE) [27], the online adaptation of control parameters F and CR is executed based on success history of these parameters in previous generations. L-SHADE [26] algorithm incorporates the linear population size reduction technique into SHADE. The population size is linearly reduced in successive generations. The steps involved in L-SHADE algorithm are briefly described in this section.

3.1. Initialization

The DE process is initialized by randomly generating a pool of candidate solutions within the defined feasible bounds (between maximum & minimum). If the initial selected population size is Np_{ini}, Np_{ini} numbers of decision vectors are created with each vector being of dimension d i.e. the dimension of the problem. A sample initialization of j-th component of the i-th decision vector can be expressed as:

$$x_{i,j}^{(0)} = x_{min,j} + rand_{i,j}[0, 1]*(x_{max,j} - x_{min,j})$$
(20)

where $rand_{i,j}[0, 1]$ is a uniformly distributed random number lying between 0 and 1 and superscript '0' represents initialization; $i = 1, 2, ..., Np_{ini}$ and $j = 1, 2, ..., d$.

3.2. Mutation

After initialization, the mutation operation produces a donor/mutant vector $v_i^{(G)}$ corresponding to each population member or target vector $x_i^{(G)}$ in the current G-th generation. L-SHADE adopts 'current-to-$p$best/1' mutation strategy defined as:

$$v_i^{(G)} = x_i^{(G)} + F_i^{(G)}\left(x_{pbest}^{(G)} - x_i^{(G)}\right) + F_i^{(G)}\left(x_{R_1^i}^{(G)} - x_{R_2^i}^{(G)}\right)$$
(21)

The mutually exclusive integers R_1^i & R_2^i are chosen randomly from the population range [1, Np]; $x_{pbest}^{(G)}$ is selected from the top $Np \times p$ ($p \in [0, 1]$, and the product is rounded up to nearest integer value) best individuals of current generation. $F_i^{(G)}$ is the positive scaling factor at generation G for the i-th individual. If an element $v_{i,j}^{(G)}$ moves outside the search range boundary $[x_{min,j}, x_{max,j}]$ during mutation, it is repaired as:

$$v_{i,j}^{(G)} = \begin{cases} \left(x_{min,j} + x_{i,j}^{(G)}\right)\big/2 \text{ if } v_{i,j}^{(G)} < x_{min,j} \\ \left(x_{max,j} + x_{i,j}^{(G)}\right)\big/2 \text{ if } v_{i,j}^{(G)} > x_{max,j} \end{cases}$$
(22)

3.3. Parameter adaptation

At generation G, each individual generates a new trial vector using its own set of parameters $F_i^{(G)}$ and $CR_i^{(G)}$. These control parameters are adapted performing the following operation:

Table 1
Electrical parameters for the PV cells at standard test conditions (STC).

Parameter	Kyocera KC200GT [36]	Shell SQ85 [23]	Shell ST40 [23]
Type	Polycrystalline	Monocrystalline	Thin film
Open circuit voltage, V_{OC} (volt)	32.9	22.20	23.30
Short circuit current, I_{SC} (amp)	8.21	5.45	2.68
Voltage at maximum power, V_{MPP} (volt)	26.3	17.20	16.60
Current at maximum power, I_{MPP} (amp)	7.61	4.95	2.41
Temperature coefficient of V_{OC}, $K_{V,OC}$ (volt/°C)	−0.123	−0.0725	−0.1
Temperature coefficient of I_{SC}, $K_{I,SC}$ (amp/°C)	3.18×10^{-3}	0.8×10^{-3}	0.35×10^{-3}
Number of cells in series, N_C	54	36	36

$$F_i^{(G)} = randc\left(\mu F_r^{(G)}, 0.1\right) \tag{23}$$

$$CR_i^{(G)} = randn\left(\mu CR_r^{(G)}, 0.1\right) \tag{24}$$

where $randc(\mu F_r^{(G)}, 0.1)$ is the value sampled from Cauchy distribution and $randn(\mu CR_r^{(G)}, 0.1)$ is the value sampled from Normal distribution. $\mu F_r^{(G)}$ is the location parameter of the Cauchy distribution, while $\mu CR_r^{(G)}$ is the mean of Normal distribution. The fixed value of 0.1 is termed as the scale parameter for Cauchy distribution and the variance for Normal distribution. The value sampled from Cauchy distribution at generation G is truncated to 1 if $F_i^{(G)} \geq 1$ or regenerated if $F_i^{(G)} \leq 0$. All μF_r and μCR_r values are initialized to 0.5 i.e. $\mu F_r^{(0)} = \mu CR_r^{(0)} = 0.5$ and updated in subsequent generations following weighted Lehmer mean [26,27].

3.4. Crossover

During crossover, the mutant vector $v_i^{(G)}$ mixes its elements with the target vector $x_i^{(G)}$ to generate the trial/offspring vector $u_i^{(G)} = (u_{i,1}^{(G)}, u_{i,2}^{(G)}, \ldots, u_{i,d}^{(G)})$. The adapted crossover rate $CR_i^{(G)}$, a value within [0,1], controls the elements which are copied from the mutant vector to the trial vector. L-SHADE employs binomial crossover and the scheme for an element is expressed as:

$$u_{i,j}^{(G)} = \begin{cases} v_{i,j}^{(G)} & \text{if } j = j_{rand} \text{ or } rand_{i,j}[0,1] \leq CR_i^{(G)}, \\ x_{i,j}^{(G)} & \text{otherwise} \end{cases} \tag{25}$$

where j_{rand} is a natural number randomly chosen in the range $[1, d]$.

3.5. Selection

Selection process compares the fitness values of the target (parent) and trial (offspring) vectors. The fitted member (with lower fitness value) moves to the next generation $G + 1$. The mathematical operation is represented as:

$$x_i^{(G+1)} = \begin{cases} u_i^{(G)} & \text{if } f\left(u_i^{(G)}\right) \leq f\left(x_i^{(G)}\right), \\ x_i^{(G)} & \text{otherwise} \end{cases} \tag{26}$$

where $f(\ldots)$ is the objective function.

3.6. Linear population size reduction (LPSR)

The success of SHADE is attributed to the online adaptation technique of scaling factor F and crossover rate CR. L-SHADE arguably improves the performance of SHADE by introducing

dynamic reduction of population size Np following a linear function. At the end of generation G, the population size for the next generation $G + 1$ becomes:

$$Np(G+1) = round\left[\left(\frac{Np_{min} - Np_{ini}}{NFE_{max}}\right)NFE + Np_{ini}\right] \tag{27}$$

As the L-SHADE mutation strategy requires minimum 4 members, Np_{min} is set to 4. NFE is the current number of fitness evaluations, while NFE_{max} is the maximum number of fitness evaluations. If $Np(G+1) < Np(G)$, the $[Np(G) - Np(G+1)]$ worst ranked individuals are deleted from the population [26]. The objective function and the selected parameters for L-SHADE algorithm are presented in section 4.

4. Objective function and application of L-SHADE algorithm

The objective of optimization is to estimate PV cell parameters accurately so that the data given in Table 1 for all three major points (open circuit, short circuit and maximum power points) are satisfied. Some of the past studies validated only the maximum power point. Here, we consider all the three points in formulation of optimization objective. Table 2 lists the details of variables to be optimized by the algorithm and also the variables that are calculated based on certain relationships described in section 2 for both single and double-diode models. In summary, diode ideality factor (a), series resistance (R_S) and parallel resistance (R_P) are optimized by the algorithm for single-diode model, while photo current (I_{PV}) and diode reverse saturation current (I_O) are derived using relationships at short circuit and open circuit points. For double-diode model, diode ideality factors (a_1, a_2), series resistance (R_S), parallel resistance (R_P) and the reverse saturation current of one diode (I_{O1}) are optimized. Photo current (I_{PV}) and reverse saturation current of second diode (I_{O2}) of the model are calculated from the optimized values of other parameters using the relationships derived in section 2. More details of the analytically calculated parameters with the relevant equation numbers are provided in Table 2.

The formulation of the objective function and its solution must ensure that the targeted performance for the PV module must conform to the I-V relationships provided at the three major points. To elaborate, the estimated parameters must generate current and voltage values of open circuit $[0, V_{OC}]$, short circuit $[I_{SC}, 0]$ and maximum power points $[I_{MPP}, V_{MPP}]$ following the I-V relationship.

Table 2
Optimized variables for different models of solar cells.

Model	Optimized parameters	Calculated parameters
Single-diode model	a, R_S, R_P	I_O [Eq. (8)], I_{PV} [Eq. (9)]
Double-diode model	$a_1, a_2, R_S, R_P, I_{O1}$	I_{O2} [Eq. (17)], I_{PV} [Eq. (18)]

The optimization algorithm is required to minimize the errors at these three points.

For single-diode model:

Error at open circuit point (from Eq. (5)):

$$err_{OC} = I_O \left[exp \left(\frac{qV_{OC}}{akN_CT} \right) - 1 \right] + \frac{V_{OC}}{R_P} - I_{PV} \tag{28}$$

Error at short circuit point (from Eq. (7)):

$$err_{SC} = I_{SC} + I_O \left[exp \left(\frac{qR_SI_{SC}}{akN_CT} \right) - 1 \right] + \frac{R_SI_{SC}}{R_P} - I_{PV} \tag{29}$$

Error at maximum power point (from Eq. (10)):

$$err_{MPP} = I_{PV} - I_O \left[exp \left(\frac{q(V_{MPP} + R_SI_{MPP})}{akN_CT} \right) - 1 \right] - \frac{V_{MPP} + R_SI_{MPP}}{R_P} - I_{MPP} \tag{30}$$

In similar manner, error values at these three points can be derived for double-diode model using Eq. (14), Eq. (16). and Eq. (19). The objective of optimization is considered as sum of the squared errors. Therefore, the algorithm shall ideally achieve zero minimum value for the aggregate error defined as:

$$ERR = err_{OC}^2 + err_{SC}^2 + err_{MPP}^2 \tag{31}$$

The user-defined inputs for the L-SHADE algorithm are provided in Table 3. For optimization cases of double-diode model, a higher number of fitness evaluations is performed due to the presence of a larger number of decision variables. L-SHADE suggested a population size of 18 times the problem dimension in Ref. [26]. However, the population sizes in Table 3 are selected after several trials to achieve good performance. The steps involved for L-SHADE algorithm in an optimization run are summarized below:

Table 3
Input parameters for L-SHADE algorithm.

Parameter	Single-diode	Double-diode
Dimension of optimization problem, d	3	5
Initial population size, Np_{ini}	50	80
Maximum no. of fitness evaluations, NFE_{max}	50,000	60,000
Decision variable range $[x_{min}, x_{max}]$	$a = [0.5, 2.0]$ $R_S = [0.001, 1]$ ohm $R_P = [50, 200]$ ohm	$a_1 = [0.5, 2.0]$ $a_2 = [0.5, 2.0]$ $I_{01} = [10^{-12}, 10^{-6}]$ amp $R_S = [0.001, 1]$ ohm $R_P = [50, 200]$ ohm

A. Input and initialization:

1. Input values of Np_{ini}, NFE_{max} (refer to Table 3).
2. Define vector x and its range $[x_{min}, x_{max}]$ for different diode-models (refer to Table 3).
3. Create random initial population of Np_{ini} such vectors defined as x_i as per Eq. (20).

4. Set generation counter $G = 0$, dynamic population size $Np(G) = Np_{ini}$, evaluation counter $NFE = 1$ and control parameters $\mu F_r^{(0)} = \mu CR_r^{(0)} = 0.5$.

B. Algorithm loop:

1. Evaluate $f(x_i^{(G)})$, i.e. '*ERR*' as per Eq. (31). for $x_i^{(G)}$ where $i = 1$ to $Np(G)$. Increase counter NFE by $Np(G)$ i.e. $NFE = NFE + Np(G)$.
2. **while** termination criteria $NFE < NFE_{max}$ **do**
3. **for** $i = 1$ to $Np(G)$ **do**
4. Adapt control parameters $F_i^{(G)}$ and $CR_i^{(G)}$ as per Eq. (23). and Eq. (24).
5. Perform mutation to generate vector $v_i^{(G)}$ as per Eq. (21). Repair if needed using Eq. (22).
6. Perform crossover to generate element $u_{i,j}^{(G)}$ as per Eq. (25). and formulate vector $u_i^{(G)}$.
7. Evaluate $f(u_i^{(G)})$ i.e. '*ERR*' as per Eq. (31). for $u_i^{(G)}$. Increase evaluation counter NFE by 1 i.e. $NFE = NFE + 1$.
8. Select the best fit individuals for next generation using Eq. (26). If, $f(u_i^{(G)}) \leq f(x_i^{(G)})$, $x_i^{(G+1)} = u_i^{(G)}$. Else $x_i^{(G+1)} = x_i^{(G)}$.
End **for** loop.
9. Update population size for next generation $Np(G+1)$ as per LPSR strategy in Eq. (27).
10. Increase generation counter $G = G+1$. Go to step 2 of algorithm loop.

The algorithm is developed using MATLAB software and simulations are performed on a computer with Intel Core i5 CPU @2.7 GHz and 4 GB RAM. Simulation results are discussed in subsequent section.

5. Simulation results and analysis

Simulation results for different solar cells with the application of L-SHADE algorithm are summarized and analyzed in this section. The case study for each of single-diode and double-diode models for every solar cell type (polycrystalline, monocrystalline and thin film) is run independently for 30 times. The optimal cell parameters for polycrystalline cell Kyocera KC200GT across 30-runs are listed in Table 4. The error function (*ERR* as per Eq. (31)) value less than 10^{-12} is treated as zero error. It is evident from the table that for numerous sets of solar cell parameters, the constraints on three major points (open circuit, short circuit and maximum power points) are all satisfied. Indeed, the parameters are different across all runs. The thirty I-V characteristics are developed and plotted in Fig. 4 corresponding to the 30-sets of optimized parameters listed in Table 4 for single-diode model of KC200GT. Following steps are implemented to develop all I-V characteristics:

1. Select a set of optimized parameters including the calculated optimal variables.
2. Discretize the voltage from 0 to V_{OC} volts in steps of 1 volt. Select maximum V as V_{OC}.
3. Calculate I value for each of the discretized V values (i.e. $V = 0$, 1, 2,…, V_{OC}) and the selected optimized parameters by solving Eq. (3). 'FSOLVE' command is used in MATLAB software.
4. As V_{MPP} is not included in the selected V values (due to fractional value of V_{MPP}), I can be separately calculated for V_{MPP}.
5. Repeat the above steps 2 to 4 for all remaining sets of optimized parameters.

As seen from Fig. 4, all the characteristics pass through the three

Table 4
Optimal parameters for single-diode model of polycrystalline PV cell, Kyocera KC200GT.

Run	Optimized variables			Calculated optimal variables		Error (ERR)
	a	R_S (ohm)	R_P (ohm)	I_O (amp)	I_{PV} (amp)	
1	1.2058	0.1969	117.0296	2.29E-08	8.2238	0
2	1.4551	0.0977	164.6476	6.71E-07	8.2149	0
3	1.1271	0.1936	86.04840	5.72E-09	8.2285	0
4	1.5030	0.0424	126.2485	1.12E-06	8.2128	0
5	1.4345	0.0852	131.4338	5.27E-07	8.2153	0
6	1.0275	0.2849	106.1348	7.52E-10	8.2320	0
7	1.3528	0.1479	157.2422	1.95E-07	8.2177	0
8	0.7939	0.4334	129.0794	8.50E-13	8.2376	0
9	1.4323	0.0923	138.2326	5.15E-07	8.2155	0
10	1.1210	0.2519	125.8930	5.18E-09	8.2264	0
11	1.2233	0.1938	123.7786	3.04E-08	8.2229	0
12	1.4547	0.0630	120.8723	6.61E-07	8.2143	0
13	1.2072	0.0991	72.25480	2.29E-08	8.2213	0
14	1.1508	0.2566	159.9519	9.02E-09	8.2232	0
15	0.9382	0.3752	177.2886	8.49E-11	8.2274	0
16	1.0946	0.2634	122.1451	3.10E-09	8.2277	0
17	1.4181	0.0959	133.4781	4.36E-07	8.2159	0
18	1.2386	0.1569	100.6933	3.83E-08	8.2228	0
19	1.2172	0.2049	132.9601	2.76E-08	8.2227	0
20	1.1207	0.2119	92.99420	5.09E-09	8.2287	0
21	1.2363	0.2095	156.5616	3.75E-08	8.2210	0
22	1.2171	0.1207	79.4578	2.70E-08	8.2225	0
23	1.2182	0.2156	150.0784	2.82E-08	8.2218	0
24	1.1812	0.2145	121.0717	1.52E-08	8.2245	0
25	1.5915	0.0390	191.5251	2.72E-06	8.2117	0
26	1.2629	0.1732	125.0325	5.57E-08	8.2214	0
27	1.1322	0.2520	134.0847	6.39E-09	8.2254	0
28	0.8697	0.2918	66.2440	1.12E-11	8.2462	0
29	1.3050	0.1719	154.6789	1.03E-07	8.2191	0
30	1.2759	0.1911	161.7367	6.80E-08	8.2197	0
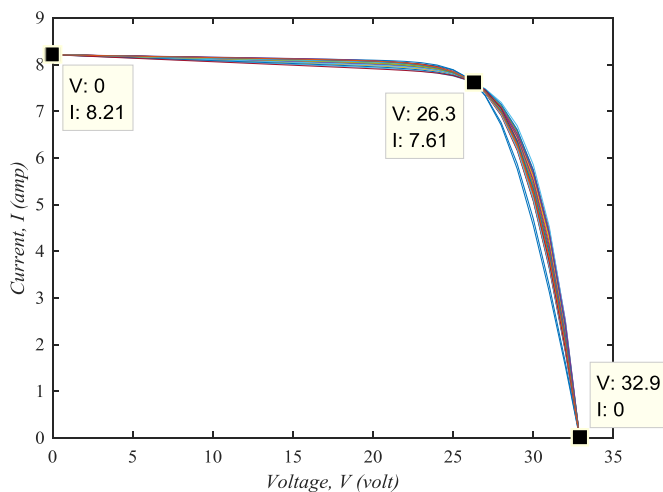
Fig. 4. 30 nos. probable I-V characteristics for single-diode model of polycrystalline cell KC200GT.

earmarked points given in Table 1 i.e.:

- Open circuit: $V = V_{OC} = 32.9$ volt, $I = 0$ amp;
- Short circuit: $V = 0$ volt, $I = I_{SC} = 8.21$ amp;
- Maximum power: $V = V_{MPP} = 26.3$ volt, $I = I_{MPP} = 7.61$ amp.

The difference in I-V characteristics can be attributed not only to different values of R_S and R_P, but also to the diode ideality factor, a. The spread (scatter) of the optimal solutions (30 sets) of these 3-

parameters is depicted in Fig. 5. It is observed that the value of each of these parameters varies over a reasonably wide range. However, each set of optimal solutions can attain zero error for the three important points. All the previous studies showed one I-V characteristic that passes through the three major points. However, the PV cell characteristic is found to be not unique when the designer focuses on the 3 points of open circuit, short circuit and maximum power. Now, the question is, does a solar cell have multiple I-V characteristics? Or does a cell have different sets of optimal parameters? In reality, a solar cell has one defined I-V characteristic corresponding to a specific set of cell parameters. But, the user can decode that specific I-V characteristic only if experimental data are available for more points and not limited to the 3-characteristic points. While estimating the optimum cell parameters, the targeted aggregate error for all available experimental I-V points shall be zero. The more the number of available I-V points, the more accurate the estimation is. Therefore, if the designer is concerned with only maximum power point, which in most cases is true, any set of optimal parameters is good enough for simulation and analysis. However, if the unique I-V characteristic and the corresponding set of cell parameters are desired, the datasheet information on three characteristic points is not sufficient and more experimental I-V data points are necessary.

The same optimization study is extended to other mono-crystalline Shell SQ85 and thin film Shell ST40 solar cells. The optimized parameters across different runs for single-diode model of Shell SQ85 PV cell are provided in Table A.1 in the Appendix. Like the earlier case with KC200GT cell, all different sets of optimal parameters are obtained in different runs leading to zero error at three major I-V points. All 30 nos. I-V characteristics are drawn in Fig. 6. As observed from the figure, all curves pass through the three defined points (marked in square boxes). The scatter of optimal solutions is plotted in Fig. 7. Variation in diode ideality factor (a) is found approximately between 1 and 1.9, while that of parallel resistance is approximately between 75 and 160 ohms. For thin film cell ST40, the optimal solutions are listed in Table A.2 in the Appendix. The multiple I-V characteristics corresponding to the optimal solution sets are provided in Fig. 8, while the optimal solutions are portrayed in 3D scatter in Fig. 9. The I-V characteristics of ST40 cell apparently show a wider spread due to the limited current capability of the thin film cell with regard to the voltage capability of the series connected cells.

The double-diode model-based solar cell parameter estimation
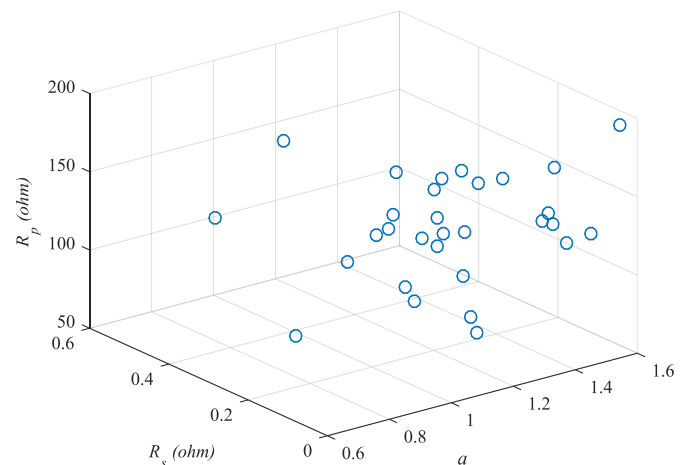
Fig. 5. Scatter of optimal solutions (30 points) for single-diode model of polycrystalline cell KC200GT.
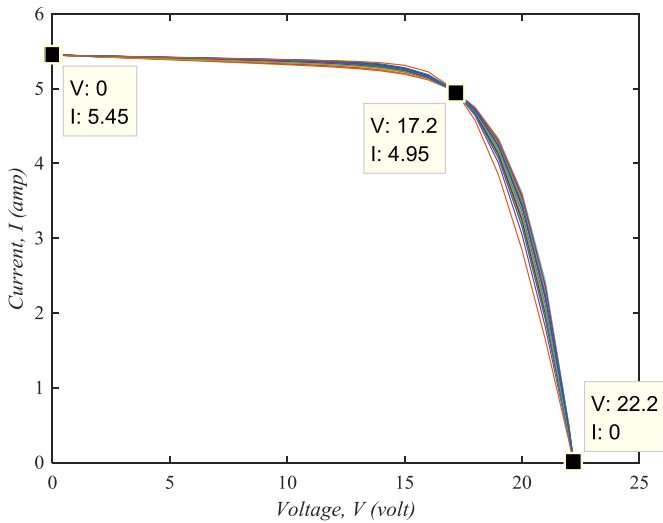
Fig. 6. 30 nos. probable I-V characteristics for single-diode model of monocrystalline cell SQ85.
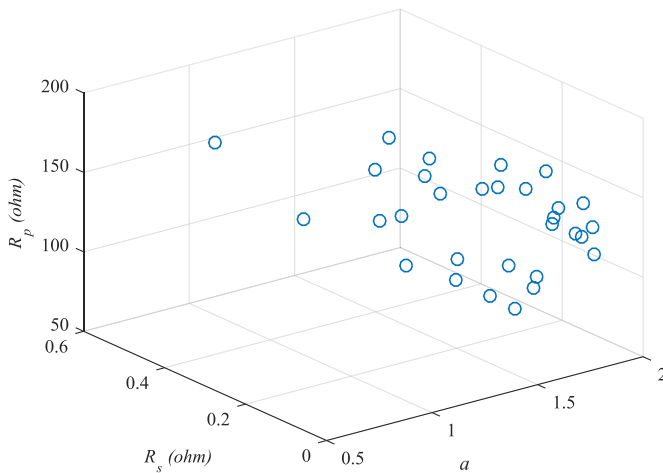

Fig. 7. Scatter of optimal solutions (30 points) for single-diode model of monocrystalline cell SQ85.
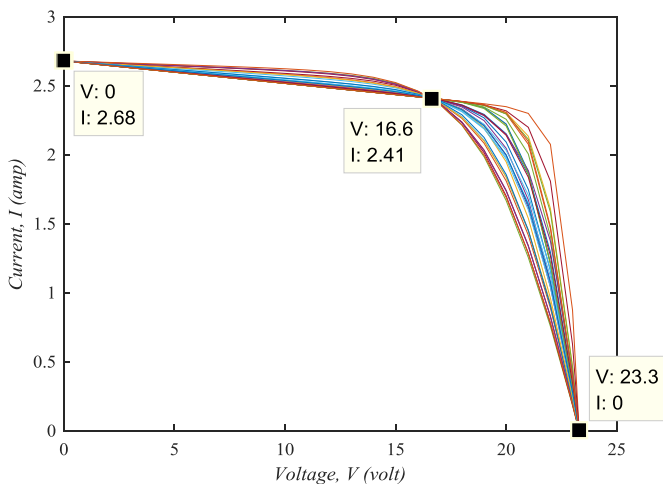

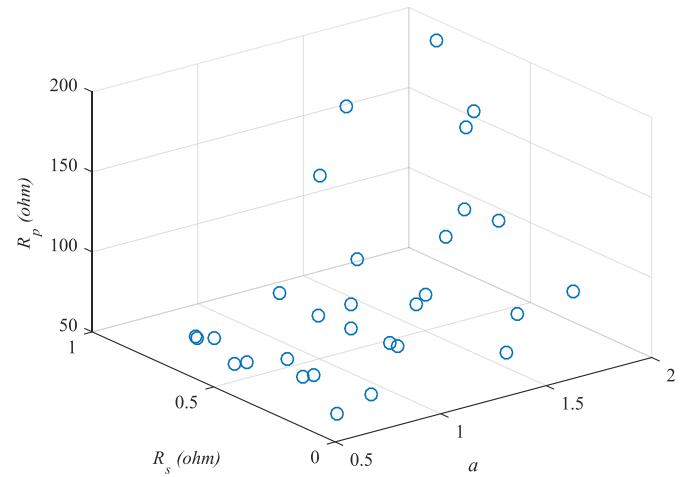**Fig. 8.** 30 nos. probable I-V characteristics for single-diode model of thin film cell ST40.

Fig. 9. Scatter of optimal solutions (30 points) for single-diode model of thin film cell ST40.

technique is known to provide a better accuracy. Therefore, parameter optimization is performed for the double-diode model of the various types of solar cells mentioned beforehand. Five variables (a_1, a_2, R_S, R_P, I_{O1}) are optimized for the double-diode adopted model, while the remaining 2 variables (I_{O2}, I_{PV}) are calculated by the relationship they share with the optimized variables. Table 5 lists the optimized parameters across different runs of the algorithm for double-diode model of polycrystalline cell KC200GT. Like single-diode model, different sets of optimized parameters result in zero error at the three major points. All the 30 I-V characteristics obtained from different sets of optimized parameters are displayed in Fig. 10. Each of the curves passes through open circuit, short circuit and maximum power points. For an easy reference and analysis of the optimized variables, the normalized values of the variables are portrayed on parallel co-ordinates plot [38] in Fig. 11. Value of R_P is found to vary over a wide range. Though I_{O1} varies from about 0.01 p.u. to 0.9 p.u., the absolute value of this diode saturation current is very small, in the range of few microampere (μA) only. The study results of the double-diode model for monocrystalline cell SQ85 and thin film cell ST40 are tabulated in Table A.3 and Table A.4, respectively, in the Appendix. The results for these PV cells can be interpreted in similar manner as the KC200GT cell. In summary, no matter whichever PV cell type we consider, or whatever PV cell parameter estimation model we adopt, we cannot obtain a unique I-V characteristic with information only about short circuit, open circuit and maximum power points. The optimization based on the 3-points can lead to different characteristics at different trials.

6. Comparative study with other metaheuristics

For a comparative study, Genetic algorithm (GA) [31], particle swarm optimization (PSO) [32], artificial bee colony (ABC) [33], moth swarm algorithm (MSA) [34] and grey wolf optimizer (GWO) [35] are applied to optimize the error objective function proposed in this work. Single and double-diode models of polycrystalline cell KC200GT are adopted for parameter optimization. Table 6 lists the user-defined control parameters selected after a few trials of each of the algorithms. It is worthwhile to note that population size is dynamic in L-SHADE algorithm. Hence, number of fitness evaluations is set as stopping criteria for the algorithm. For the remaining

Table 5
Optimal parameters for double-diode model of polycrystalline PV cell, Kyocera KC200GT.

Run	Optimized variables					Calculated optimal variables		Error (ERR)
	a_1	a_2	R_S (ohm)	R_P (ohm)	I_{O1} (amp)	I_{O2} (amp)	I_{PV} (amp)	
1	1.8433	1.5196	0.0488	150.8207	6.66E-07	1.29E-06	8.2127	0
2	1.9109	1.5752	0.0322	162.6718	1.37E-07	2.31E-06	8.2116	0
3	1.7967	0.8279	0.4096	120.6687	2.50E-09	2.89E-12	8.2379	0
4	1.6179	0.8729	0.3132	95.57680	2.97E-07	1.15E-11	8.2369	0
5	1.8518	1.4143	0.1294	192.5573	1.92E-07	4.17E-07	8.2155	0
6	1.6979	1.3323	0.1584	181.2867	3.90E-07	1.41E-07	8.2172	0
7	1.6514	1.0740	0.2060	121.4418	8.50E-07	1.67E-09	8.2239	0
8	1.9925	0.9587	0.3262	114.6097	4.80E-07	1.42E-10	8.2334	0
9	1.7462	1.1150	0.2360	118.6523	3.19E-07	4.46E-09	8.2263	0
10	1.6639	1.0872	0.2606	134.9574	2.37E-07	2.56E-09	8.2259	0
11	1.5655	1.2624	0.1479	119.6371	2.32E-07	4.91E-08	8.2201	0
12	1.7419	1.2627	0.1599	122.0194	3.41E-07	5.36E-08	8.2208	0
13	1.8023	1.1142	0.1461	76.2376	7.57E-07	4.23E-09	8.2257	0
14	1.9042	1.0676	0.2536	100.4639	6.39E-08	1.78E-09	8.2307	0
15	1.4100	0.8923	0.2892	121.2395	1.01E-07	1.70E-11	8.2296	0
16	1.7000	1.3175	0.1496	143.4129	2.65E-07	1.17E-07	8.2186	0
17	1.6781	1.2195	0.1812	125.4525	3.31E-07	2.69E-08	8.2219	0
18	1.6734	1.3341	0.1145	122.3676	4.58E-07	1.39E-07	8.2177	0
19	1.7198	0.9602	0.2996	127.8893	6.96E-07	1.37E-10	8.2292	0
20	1.7148	1.1798	0.2336	160.1328	1.92E-07	1.46E-08	8.2220	0
21	1.7018	1.0946	0.2247	102.3364	2.92E-07	2.96E-09	8.2280	0
22	1.5315	1.3250	0.0941	115.7357	4.30E-07	9.55E-08	8.2167	0
23	1.8548	1.3424	0.1338	135.4045	3.55E-07	1.67E-07	8.2181	0
24	1.5236	1.2473	0.0599	87.0126	4.91E-07	2.78E-08	8.2156	0
25	1.9312	1.1642	0.2437	155.5184	2.92E-07	1.13E-08	8.2229	0
26	1.8167	1.5035	0.0393	125.7689	2.11E-07	1.11E-06	8.2126	0
27	1.6244	0.7554	0.3356	173.1607	8.83E-07	1.42E-13	8.2259	0
28	1.7809	1.0721	0.2289	90.8337	1.90E-07	1.92E-09	8.2307	0
29	1.9518	1.1876	0.1972	112.1273	3.67E-07	1.67E-08	8.2244	0
30	1.9267	1.2499	0.1343	96.5488	6.76E-07	4.45E-08	8.2214	0
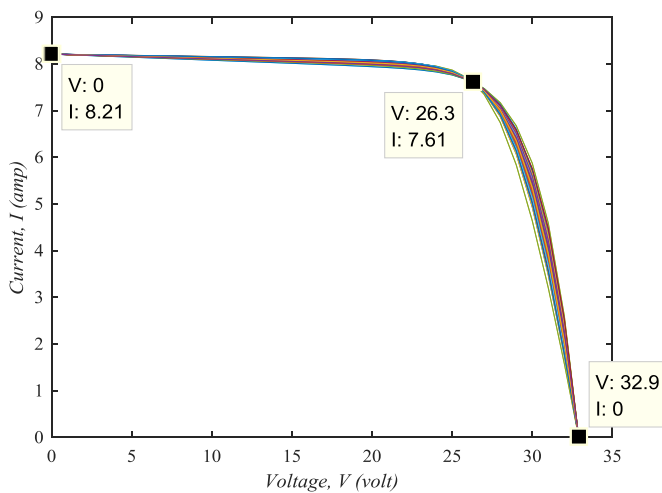
Fig. 10. 30 nos. probable I-V characteristics for double-diode model of polycrystalline cell KC200GT.
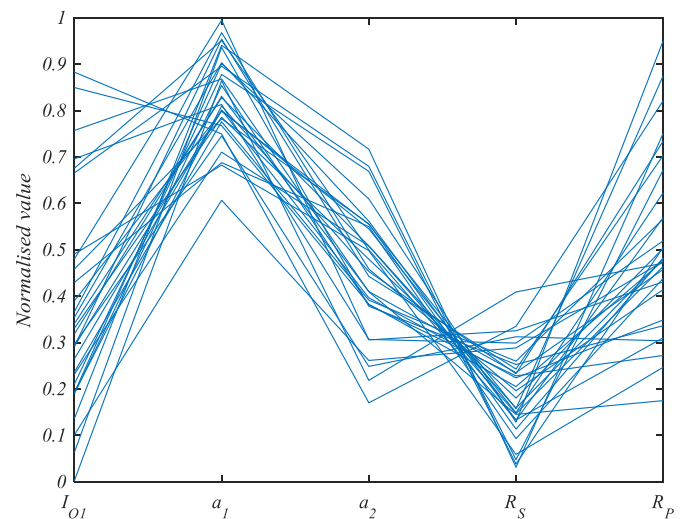
Fig. 11. Parallel co-ordinates plot of optimal solutions for double-diode model of polycrystalline cell KC200GT.

algorithms, the selected numbers of iterations are equivalent to the number of fitness evaluations in L-SHADE as in each iteration 'Np' (population size) numbers of fitness evaluations are performed. Further, instead of static inertia weight in PSO, we choose dynamic inertia weight where the inertia weight changes as the iteration progresses in pursuit of optimal solutions. The inertia weight w at iteration I changes following the relationship:

$$w = w_{max} - I \times \frac{w_{max} - w_{min}}{I_{max}} \tag{32}$$

where I_{max} is the maximum number of iterations, w_{max} and w_{min} are the selected maximum and minimum inertia weights. Each algorithm is run 30 times with the final values of the selected control parameters. A statistical summary of the objective function

Table 6
Control parameters of various optimization algorithms for KC200GT cell parameter estimation.

| Algorithm	Control parameter description	Values of control parameters	
		Single-diode	Double-diode
GA	Mutation rate (μ)	0.1	0.1
	Crossover probability (CR)	0.9	0.9
	Population size (Np)	50	50
	Maximum number of iterations	1000	1200
PSO	Max inertia weight (w_{max})	0.9	0.9
	Min inertia weight (w_{min})	0.4	0.4
	Cognitive learning factor (c_1)	2	2
	Social learning factor (c_2)	2	2
	Population size (Np)	50	50
	Maximum number of iterations	1000	1200
ABC	Number of onlooker bees	50	50
	Population size (Np)	50	50
	Maximum number of iterations	1000	1200
MSA	Number of search agents (Np)	50	50
	Number of pathfinders	6	6
	Maximum number of iterations	1000	1200
GWO	Number of search agents (Np)	50	50
	Maximum number of iterations	1000	1200
L-SHADE	Initial population size (Np_{ini})	50	80
	Maximum number of fitness evaluations	50000	60000

Table 7
Statistical summary of case studies with polycrystalline KC200GT cell using various algorithms.

Case no.	Algorithm	Error function (ERR)				Total CPU time (sec.)
		Best	Worst	Mean	Std. dev.	
KC200GT (Single-diode model)	GA	0	0	0	0	70.6
	PSO	0	0	0	0	18.1
	ABC	0	5.61×10^{-11}	4.73×10^{-12}	1.19×10^{-11}	110.3
	MSA	0	0	0	0	50.8
	GWO	0	2.79×10^{-11}	5.27×10^{-12}	7.80×10^{-12}	8.2
	L-SHADE	0	0	0	0	17.9
KC200GT (Double-diode model)	GA	0	0	0	0	85.5
	PSO	0	0	0	0	21.7
	ABC	0	5.79×10^{-11}	4.84×10^{-12}	1.05×10^{-11}	150.7
	MSA	0	0	0	0	65.4
	GWO	0	9.86×10^{-11}	5.51×10^{-12}	1.82×10^{-11}	10.9
	L-SHADE	0	0	0	0	18.6
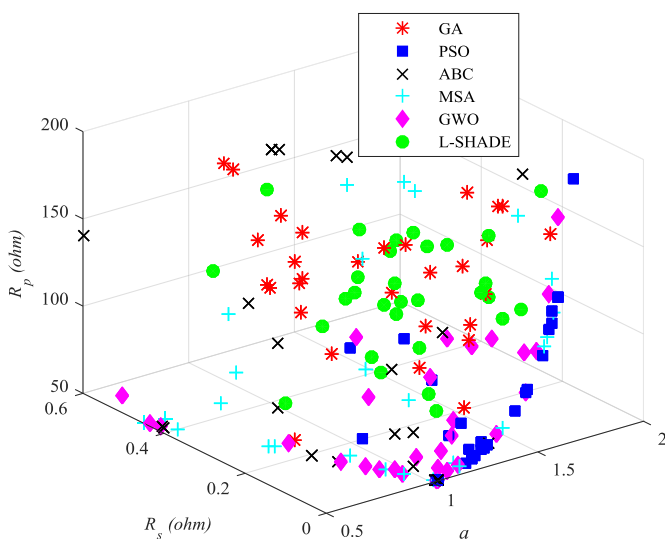
Fig. 12. Scatter of optimal solutions for single-diode model of KC200GT cell using various algorithms.

value is presented in Table 7.

As observed from Table 7, algorithms GA, PSO, MSA and L-SHADE could obtain zero error across all trial runs. The worst error values for ABC and GWO algorithms are in the order of 10^{-11}. This error can also be treated as zero for all practical applications. The optimal values of the cell parameters for all the algorithms across all 30 trial runs (total $30 \times 6 = 180$ points) are shown in 3D scatter plot in Fig. 12. It can be inferred that irrespective of the algorithm employed, the targeted performance of the solar cell can be achieved at three major points of short circuit, open circuit and maximum power with different sets of cell parameters. The 'total CPU time' in Table 7 is the time required to execute all 30 runs of the respective algorithm. GWO appears to be the fastest followed by L-SHADE and PSO algorithms. However, an interesting point to note here is that the solutions proposed by both GWO and PSO are more concentrated and not well spread unlike other algorithms as seen in Fig. 12. This very fact implies the limited exploration capability of these two algorithms. Nonetheless, the objective of current study is not to claim superiority of any algorithm over the other, but to point out to the fact that datasheet information of only on three major points of a solar cell is insufficient to find out its unique I-V characteristic.

7. Conclusion

This paper presents parameter estimation of PV cells by applying some selected evolutionary algorithms with the use of datasheet information at three major points of I-V characteristic: open circuit, short circuit and maximum power points. Parameter optimizations adopting single-diode and double-diode models for different types of PV cells are performed in this study. Detailed circuit analyses are presented for both single-diode and double-diode models, and parameters are extracted partly by analytical method and partly by the optimization algorithms. While application of L-SHADE algorithm is presented in detail, the results obtained using algorithms such as GA, PSO, ABC, MSA and GWO are succinctly exhibited. It is substantiated with simulation and analysis that a unique I-V characteristic cannot be attained with limited datasheet information of only on the three major points. Different sets of probable optimal parameters can satisfy the I-V relationships at the three points. Hence, importance only on all or one of the 3-points allows the designer to choose any optimal set of parameters from the pool of optimized solutions. In order to obtain a unique and accurate I-V characteristic of a PV cell, experimental data on more points (definitely more than 3-major points) are necessary. Although the study is performed at STC condition for the PV cells, the conclusion is valid for other temperatures and irradiance levels. At any other temperature or irradiance level, multiple sets of optimal parameters can be obtained at different trial runs and each set of parameters can conform to the I-V relationships at the three major points.

Acknowledgement

Appendix

Table A.1
Optimal parameters for single-diode model of monocrystalline PV cell, Shell SQ85.

Run	Optimized variables			Calculated optimal variables		Error (*ERR*)
	a	R_S (ohm)	R_P (ohm)	I_O (amp)	I_{PV} (amp)	
1	1.8760	0.0850	140.9505	1.47E-05	5.4533	0
2	1.6884	0.1886	160.4777	3.56E-06	5.4564	0
3	1.3681	0.3229	120.8985	1.27E-07	5.4646	0
4	1.8148	0.1126	137.3839	9.55E-06	5.4545	0
5	1.5298	0.2552	139.8978	8.14E-07	5.4599	0
6	1.8883	0.0683	128.0143	1.59E-05	5.4529	0
7	1.6987	0.1148	90.4292	3.81E-06	5.4569	0
8	1.7975	0.1161	130.9026	8.39E-06	5.4548	0
9	1.5859	0.1624	84.5502	1.39E-06	5.4605	0
10	1.8578	0.0776	121.8453	1.29E-05	5.4535	0
11	1.1842	0.4134	118.0667	8.33E-09	5.4691	0
12	1.7939	0.1152	127.7473	8.16E-06	5.4549	0
13	1.4247	0.2973	124.6888	2.55E-07	5.4630	0
14	1.5183	0.2107	90.7676	7.11E-07	5.4626	0
15	1.4953	0.2776	149.8543	5.68E-07	5.4601	0
16	1.5385	0.2175	102.2491	8.80E-07	5.4616	0
17	1.3763	0.3366	151.2183	1.42E-07	5.4621	0
18	1.6329	0.2073	144.7247	2.19E-06	5.4578	0
19	1.6605	0.1533	101.3474	2.76E-06	5.4582	0
20	1.8762	0.0568	111.8192	1.46E-05	5.4528	0
21	1.5115	0.2749	160.8947	6.76E-07	5.4593	0
22	1.4193	0.3237	171.4422	2.41E-07	5.4603	0
23	1.6297	0.1246	78.8210	2.08E-06	5.4586	0
24	1.7166	0.1171	96.8097	4.43E-06	5.4566	0
25	1.8441	0.0858	123.1616	1.17E-05	5.4538	0
26	1.4075	0.2776	96.4558	2.06E-07	5.4657	0
27	1.6744	0.1879	146.4434	3.16E-06	5.4570	0
28	1.7413	0.1555	147.1881	5.48E-06	5.4558	0
29	1.7987	0.1339	158.6289	8.52E-06	5.4546	0
30	0.9867	0.5298	159.2777	1.45E-10	5.4681	0

Table A.2
Optimal parameters for single-diode model of thin-film PV cell, Shell ST40.

Run	Optimized variables			Calculated optimal variables		Error (ERR)
	a	R_S (ohm)	R_P (ohm)	I_O (amp)	I_{PV} (amp)	
1	1.1511	0.4982	64.1566	7.33E-10	2.7008	0
2	1.8294	0.6214	105.585	2.59E-06	2.6958	0
3	0.7174	0.3232	61.2282	1.30E-15	2.6941	0
4	1.2643	0.5998	67.4728	5.24E-09	2.7038	0
5	1.6910	0.9883	149.4855	8.62E-07	2.6977	0
6	1.7302	0.6131	93.1849	1.16E-06	2.6976	0
7	1.5597	0.9835	111.9217	2.41E-07	2.7036	0
8	1.1786	0.3304	63.5887	1.21E-09	2.6939	0
9	0.6415	0.4868	61.0419	2.05E-17	2.7014	0
10	0.6571	0.7136	60.9131	5.23E-17	2.7114	0
11	1.1279	0.6118	64.6170	4.68E-10	2.7054	0
12	0.7625	0.3133	61.2828	1.04E-14	2.6937	0
13	1.6438	0.2424	72.6505	5.23E-07	2.6889	0
14	1.9412	0.7136	146.7342	5.86E-06	2.6930	0
15	0.6562	0.7043	60.9154	4.94E-17	2.7110	0
16	0.5741	0.0543	61.4294	2.02E-19	2.6824	0
17	1.8872	0.5319	103.3401	3.94E-06	2.6938	0
18	1.9711	0.7104	156.0223	7.16E-06	2.6922	0
19	0.7858	0.4464	61.2645	2.77E-14	2.6995	0
20	1.8679	0.2081	81.2480	3.34E-06	2.6869	0
21	0.7951	0.1085	61.4558	4.01E-14	2.6847	0
22	1.4589	0.7394	79.2321	7.65E-08	2.7050	0
23	1.9324	0.8297	193.3936	5.61E-06	2.6915	0
24	1.1393	0.7844	66.7870	5.90E-10	2.7115	0
25	1.4305	0.1046	65.7126	5.24E-08	2.6843	0
26	0.7080	0.6789	61.0332	8.21E-16	2.7098	0
27	1.4966	0.4905	72.9187	1.16E-07	2.6980	0
28	1.1752	0.3608	63.6942	1.14E-09	2.6952	0
29	1.4319	0.4757	70.3107	5.42E-08	2.6981	0
30	0.5997	0.5016	61.0062	1.32E-18	2.7020	0

Table A.3
Optimal parameters for double-diode model of monocrystalline PV cell, Shell SQ85.

Run	Optimized variables					Calculated optimal variables		Error (ERR)
	a_1	a_2	R_S (ohm)	R_P (ohm)	I_{O1} (amp)	I_{O2} (amp)	I_{PV} (amp)	
1	1.7801	1.6356	0.0797	67.1105	1.46E-08	2.17E-06	5.4565	0
2	1.8850	1.7283	0.1222	105.0533	2.41E-07	4.81E-06	5.4563	0
3	1.9220	1.3533	0.2691	79.1226	3.79E-07	1.01E-07	5.4685	0
4	1.6887	1.3038	0.1614	54.9977	6.02E-07	4.21E-08	5.4660	0
5	1.7724	1.8279	0.0767	106.5154	5.48E-07	9.58E-06	5.4539	0
6	1.8507	1.8353	0.0550	96.8293	3.36E-07	1.06E-05	5.4531	0
7	1.8706	1.8469	0.1218	185.1248	9.18E-07	1.13E-05	5.4536	0
8	1.9168	1.8224	0.1230	162.5228	5.94E-07	9.83E-06	5.4541	0
9	1.6780	1.3580	0.3099	122.5154	3.69E-07	9.87E-08	5.4638	0
10	1.8640	1.7755	0.0857	98.1603	8.47E-07	6.59E-06	5.4548	0
11	1.9034	1.8958	0.0865	158.5245	1.09E-07	1.68E-05	5.4530	0
12	1.6000	1.6017	0.2217	142.9849	1.68E-07	1.48E-06	5.4585	0
13	1.8984	1.9061	0.0705	141.2452	6.49E-07	1.73E-05	5.4527	0
14	1.8088	1.7788	0.1230	128.8713	4.33E-07	6.95E-06	5.4552	0
15	1.7676	1.7478	0.1400	131.4551	8.65E-07	5.00E-06	5.4558	0
16	1.9255	1.7736	0.1259	132.6791	9.50E-07	6.69E-06	5.4552	0
17	1.8617	1.5541	0.2008	99.8431	4.22E-07	9.95E-07	5.4610	0
18	1.6853	1.6712	0.1568	109.1195	5.42E-07	2.56E-06	5.4578	0
19	1.7173	1.6806	0.1342	96.9424	4.18E-07	2.97E-06	5.4575	0
20	1.7824	1.8297	0.1199	158.5669	3.80E-07	1.01E-05	5.4541	0
21	1.5585	1.3653	0.1467	60.9686	5.37E-07	5.75E-08	5.4631	0
22	1.8657	1.9036	0.0187	95.9415	5.10E-07	1.68E-05	5.4511	0
23	1.7949	1.7979	0.1197	135.5270	6.21E-07	7.79E-06	5.4548	0
24	1.5485	1.4453	0.2648	114.2090	2.47E-07	2.41E-07	5.4626	0
25	1.6560	1.7532	0.1727	183.8524	3.30E-07	5.31E-06	5.4551	0
26	1.8700	1.6898	0.1723	141.4586	7.53E-07	3.40E-06	5.4566	0
27	1.7410	1.4317	0.2592	99.4174	3.10E-07	2.59E-07	5.4642	0
28	1.8105	1.5237	0.2430	132.0920	6.31E-07	7.11E-07	5.4600	0
29	1.7946	1.6643	0.2043	172.9946	1.90E-07	2.84E-06	5.4564	0
30	1.8152	1.2823	0.3677	174.2476	8.18E-07	3.63E-08	5.4615	0

Table A.4
Optimal parameters for double-diode model of thin-film PV cell, Shell ST40.

Run	Optimized variables					Calculated optimal variables		Error (ERR)
	a_1	a_2	R_S (ohm)	R_P (ohm)	I_{O1} (amp)	I_{O2} (amp)	I_{PV} (amp)	
1	1.9065	1.9250	0.7522	153.0828	3.91E-07	4.82E-06	2.6932	0
2	1.8842	1.5713	0.7022	85.2624	5.20E-09	2.64E-07	2.7021	0
3	1.8206	1.8651	0.8217	153.2414	3.94E-07	2.91E-06	2.6944	0
4	1.6633	1.6645	0.5843	85.6029	2.50E-07	3.97E-07	2.6983	0
5	1.7872	1.6424	0.4010	76.7627	2.69E-08	5.14E-07	2.6940	0
6	1.7654	0.5556	0.2804	61.8243	6.88E-08	4.50E-20	2.6922	0
7	1.7827	1.7803	0.3720	82.9629	3.12E-07	1.42E-06	2.6920	0
8	1.9481	1.9393	0.3139	91.0962	7.28E-07	4.87E-06	2.6892	0
9	1.7463	1.5243	0.2691	73.3629	6.72E-07	7.54E-08	2.6898	0
10	1.8744	0.9899	0.2629	61.9698	1.02E-08	2.05E-11	2.6914	0
11	1.8786	1.5824	0.4708	76.8469	1.83E-07	2.77E-07	2.6964	0
12	1.8334	1.9087	0.6337	118.7946	3.00E-07	4.12E-06	2.6943	0
13	1.7719	1.6087	0.4246	76.8313	1.98E-07	3.31E-07	2.6948	0
14	1.6865	1.6602	0.6929	93.3649	2.66E-07	4.20E-07	2.6999	0
15	1.9999	1.8601	0.6178	111.4634	6.91E-07	3.00E-06	2.6949	0
16	1.8505	0.9445	0.2214	64.0935	4.61E-07	5.09E-12	2.6893	0
17	1.7570	1.7569	0.6505	99.3375	1.11E-07	1.35E-06	2.6976	0
18	1.6729	1.6724	0.9111	122.5050	1.96E-07	5.26E-07	2.6999	0
19	1.8204	1.8821	0.5948	109.8278	3.64E-08	3.76E-06	2.6945	0
20	1.8917	1.8641	0.1001	77.7228	6.09E-07	2.72E-06	2.6835	0
21	1.8190	1.8148	0.3729	85.2798	8.42E-07	1.45E-06	2.6917	0
22	1.7118	1.7139	0.5719	88.6591	8.75E-07	1.17E-07	2.6973	0
23	1.8493	1.6547	0.9511	127.7029	4.38E-08	6.07E-07	2.7000	0
24	1.8135	1.7034	0.8434	116.9312	6.80E-08	9.17E-07	2.6993	0
25	1.7555	1.6290	0.7303	99.7499	7.38E-07	2.32E-07	2.6996	0
26	1.8962	1.8917	0.6130	114.0591	2.95E-07	3.81E-06	2.6944	0
27	1.8471	1.6204	0.8066	102.8662	4.29E-07	3.75E-06	2.7010	0
28	1.8505	1.7782	0.8410	134.1845	1.38E-07	1.70E-06	2.6968	0
29	1.8732	1.7878	0.5527	94.8400	2.77E-07	1.72E-06	2.6956	0
30	1.6848	1.5866	0.1409	70.4268	3.37E-07	1.66E-07	2.6854	0

References

[1] M.K. Deshmukh, S.S. Deshmukh, Modeling of hybrid renewable energy systems, Renew. Sustain. Energy Rev. 12 (no. 1) (2008) 235−249.

[2] Kashif Ishaque, Zainal Salam, Hamed Taheri, Simple, fast and accurate two-diode model for photovoltaic modules, Sol. Energy Mater. Sol. Cells 95 (2) (2011) 586−594.

[3] Dalia Allam, D.A. Yousri, M.B. Eteiba, Parameters extraction of the three-diode model for the multi-crystalline solar cell/module using Moth-Flame Optimization Algorithm, Energy Convers. Manag. 123 (2016) 535−548.

[4] Vandana Khanna, B.K. Das, Dinesh Bisht, P.K. Singh, A three-diode model for industrial solar cells and estimation of solar cell parameters using PSO algorithm, Renew. Energy 78 (2015) 105−113.

[5] A. Rezaee Jordehi, Parameter estimation of solar photovoltaic (PV) cells: a review, Renew. Sustain. Energy Rev. 61 (2016) 354−371.

[6] A. Rezaee Jordehi, Time varying acceleration coefficients particle swarm optimisation (TVACPSO): a new optimisation algorithm for estimating parameters of PV cells and modules, Energy Convers. Manag. 129 (2016) 262−274.

[7] A. Rezaee Jordehi, Enhanced leader particle swarm optimisation (ELPSO): an efficient algorithm for parameter estimation of photovoltaic (PV) cells and modules, Sol. Energy 159 (2018) 78−87.

[8] D.F. Alam, D.A. Yousri, M.B. Eteiba, Flower pollination algorithm based solar PV parameter estimation, Energy Convers. Manag. 101 (2015) 410−422.

[9] Shuhui Xu, Yong Wang, Parameter estimation of photovoltaic modules using a hybrid flower pollination algorithm, Energy Convers. Manag. 144 (2017) 53−68.

[10] Xiankun Gao, Yan Cui, Jianjun Hu, Guangyin Xu, Zhenfeng Wang, Jianhua Qu, Heng Wang, Parameter extraction of solar cell models using improved shuffled complex evolution algorithm, Energy Convers. Manag. 157 (2018) 460−479.

[11] Kunjie Yu, J.J. Liang, B.Y. Qu, Xu Chen, Heshan Wang, Parameters identification of photovoltaic models using an improved JAYA optimization algorithm, Energy Convers. Manag. 150 (2017) 742−753.

[12] Wenyin Gong, Zhihua Cai, Parameter extraction of solar cell models using repaired adaptive differential evolution, Sol. Energy 94 (2013) 209−220.

[13] Lian Lian Jiang, Douglas L. Maskell, Jagdish C. Patra, Parameter estimation of solar cells and modules using an improved adaptive differential evolution algorithm, Appl. Energy 112 (2013) 185−193.

[14] Diego Oliva, Mohamed Abd El Aziz, Aboul Ella Hassanien, Parameter estimation of photovoltaic cells using an improved chaotic whale optimization algorithm, Appl. Energy 200 (2017) 141−154.

[15] T. Easwarakhanthan, J. Bottin, I. Bouhouch, C. Boutrit, Nonlinear minimization algorithm for determining the solar cell parameters with microcomputers, Int. J. Sol. Energy 4 (1) (1986) 1−12.

[16] Kashif Ishaque, Zainal Salam, Saad Mekhilef, Amir Shamsudin, Parameter extraction of solar photovoltaic modules using penalty-based differential evolution, Appl. Energy 99 (2012) 297−308.

[17] Dhiaa Halboot Muhsen, Abu Bakar Ghazali, Tamer Khatib, Issa Ahmed Abed, Parameters extraction of double diode photovoltaic module's model based on hybrid evolutionary algorithm, Energy Convers. Manag. 105 (2015) 552−561.

[18] Bidyadhar Subudhi, Raseswari Pradhan, Bacterial foraging optimization approach to parameter extraction of a photovoltaic module, IEEE Trans. Sustain. Energy 9 (1) (2018) 381−389.

[19] Ahmed Fathy, Hegazy Rezk, Parameter estimation of photovoltaic system using imperialist competitive algorithm, Renew. Energy 111 (2017) 307−320.

[20] K. Et-torabi, I. Nassar-eddine, A. Obbadi, Y. Errami, R. Rmaily, S. Sahnoun, M. Agunaou, Parameters estimation of the single and double diode photovoltaic models using a Gauss−Seidel algorithm and analytical method: a comparative study, Energy Convers. Manag. 148 (2017) 1041−1054.

[21] I. Nassar-Eddine, A. Obbadi, Y. Errami, M. Agunaou, Parameter estimation of photovoltaic modules using iterative method and the Lambert W function: a comparative study, Energy Convers. Manag. 119 (2016) 37−48.

[22] Marcelo Gradella Villalva, Jonas Rafael Gazoli, Ernesto Ruppert Filho, Comprehensive approach to modeling and simulation of photovoltaic arrays, IEEE Trans. Power Electron. 24 (5) (2009) 1198−1208.

[23] Jing Jun Soon, Kay-Soon Low, Photovoltaic model identification using particle swarm optimization with inverse barrier constraint, IEEE Trans. Power Electron. 27 (9) (2012) 3975−3983.

[24] M.S. Ismail, M. Moghavvemi, T.M.I. Mahlia, Characterization of PV panel and global optimization of its model parameters using genetic algorithm, Energy Convers. Manag. 73 (2013) 10−25.

[25] Mohamed A. Awadallah, Variations of the bacterial foraging algorithm for the extraction of PV module parameters from nameplate data, Energy Convers. Manag. 113 (2016) 312−320.

[26] Ryoji Tanabe, Alex Fukunaga, Improving the search performance of SHADE using linear population size reduction, in: Evolutionary Computation (CEC), 2014 IEEE Congress on, IEEE, 2014, pp. 1658−1665.

[27] Ryoji Tanabe, Alex Fukunaga, Success-history based parameter adaptation for differential evolution, in: Evolutionary Computation (CEC), 2013 IEEE Congress on, IEEE, 2013, pp. 71−78.

[28] Partha P. Biswas, P.N. Suganthan, Gehan AJ. Amaratunga, Optimal placement of wind turbines in a windfarm using L-SHADE algorithm, in: Evolutionary Computation (CEC), 2017 IEEE Congress on, IEEE, 2017, pp. 83−88.

[29] Partha P. Biswas, P.N. Suganthan, Gehan AJ. Amaratunga, Minimizing harmonic distortion in power system with optimal design of hybrid active power

filter using differential evolution, Appl. Soft Comput. 61 (2017) 486—496.

[30] Partha P. Biswas, P.N. Suganthan, Gehan AJ. Amaratunga, Optimal power flow solutions incorporating stochastic wind and solar power, Energy Convers. Manag. 148 (2017) 1194—1207.

[31] John H. Holland, Adaptation in Natural and Artificial Systems: an Introductory Analysis with Applications to Biology, Control, and Artificial Intelligence, MIT press, 1992.

[32] James Kennedy, Eberhart Russell, Particle swarm optimization, in: Neural Networks, 1995. Proceedings., IEEE International Conference on vol. 4, IEEE, 1995.

[33] Dervis Karaboga, Technical report-tr06, An Idea Based on Honey Bee Swarm for Numerical Optimization, vol. 200, Erciyes University, Engineering Faculty, Computer Engineering Department, 2005.

[34] Al-Attar Ali Mohamed, Yahia S. Mohamed, Ahmed AM. El-Gaafary, Ashraf M. Hemeida, Optimal power flow using moth swarm algorithm, Elec. Power Syst. Res. 142 (2017) 190—206.

[35] Seyedali Mirjalili, Seyed Mohammad Mirjalili, Andrew Lewis, Grey wolf optimizer, Adv. Eng. Software 69 (2014) 46—61.

[36] KC200GT High Efficiency Multicrystal Photovoltaic Module Datasheet Kyocera. [Online]. Available: http://www.kyocerasolar.com/assets/001/5195.pdf.

[37] R. Mallipeddi, P.N. Suganthan, Q.K. Pan, M.F. Tasgetiren, Differential evolution algorithm with ensemble of parameters and mutation strategies, Appl. Soft Comput. 11 (2) (2011) 1679—1696.

[38] A. Inselberg, B. Dimsdale, Parallel coordinates for visualizing multi-dimensional geometry, in: Computer Graphics 1987, Springer, Tokyo, 1987, pp. 25—44.